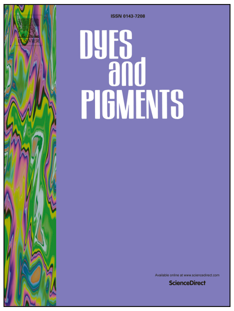

Synthesis and properties of photochromic spirooxazine with aggregation-induced emission fluorophores polymeric nanoparticles

Xue Li, Chengpeng Li, Sheng Wang, Huan Dong, Xiang Ma, Derong Cao

PII: S0143-7208(17)30311-X
DOI: 10.1016/j.dyepig.2017.03.068
Reference: DYPI 5906

To appear in: *Dyes and Pigments*

Received Date: 16 February 2017
Revised Date: 13 March 2017
Accepted Date: 18 March 2017

Please cite this article as: Li X, Li C, Wang S, Dong H, Ma X, Cao D, Synthesis and properties of photochromic spirooxazine with aggregation-induced emission fluorophores polymeric nanoparticles, *Dyes and Pigments* (2017), doi: 10.1016/j.dyepig.2017.03.068.

Synthesis and Properties of Photochromic Spirooxazine with Aggregation-Induce Emission Fluorophores polymeric nanoparticles

Xue Li[a,b], Chengpeng Li[b], Sheng Wang[a,b,]*, Huan Dong[c], Xiang Ma[c,]**, Derong Cao[a,]**

[a] *School of Chemistry and Chemical Engineering, State Key Laboratory of Luminescent Materials and Devices, South China University of Technology, Guangzhou 510641, China*
[b] *School of Chemistry and Chemical Engineering, Development Center for New Materials Engineering & Technology in Universities of Guangdong, Lingnan Normal University, Zhanjiang 524048, China*
[c] *Key Laboratory for Advanced Materials and Institute of Fine Chemicals, East China University of Science and Technology*
Meilong Road 130, Shanghai, 200237, P. R. China

**Corresponding author: Prof. Dr. Sheng Wang, School of Chemistry & Chemical Engineering, Lingnan Normal University, Zhanjiang 524048, P.R. China; Tel: +86-759-318-2515; Fax: +86-759-318-3510; E-mail: dyesws@126.com;*
Prof. Dr. Derong Cao, State Key Laboratory of Luminescent Materials and Devices, South China University of Technology, Guangzhou 510641, P.R. China; Tel: +86-020-8711-0245; Fax: +86-020-8711-0245; E-mail: drcao@scut.edu.cn;
Prof. Dr. Xiang Ma, Key Laboratory for Advanced Materials and Institute of Fine Chemicals, East China University of Science and Technology
Meilong Road 130, Shanghai, 200237, P. R. China; Tel: +86-21-64252288, Fax: +86-21-64252288; E-mail: maxiang@ecust.edu.cn

Abstract: We designed and synthesized photochromic fluorescent poly (MMA-co-SPO-co-TPE) nanoparticles with pendant spirooxazine (SPO) dye and tetraphenylethylene (TPE) fuorophores attached to poly (methyl methacrylate) (MMA) backbone by semi-continuous polymerization. The polymerization reactions were accomplished in water with randomly methylated-β-cyclodextrin (β-CD) at 80℃ in the presence of potassium peroxodisulfate which can be used as free radical initiator. This new synthetic method leads to uniform and smooth nanoparticles with a narrow particle size distribution. In addition, the poly (MMA-co-SPO-co-TPE) nanoparticles exhibit aggregation induced emission (AIE) properties and excellent photochemical properties because of spirooxazine dyes convert reversibly to merocyanine form upon ultraviolet (UV) irradiation, which active the intramolecular energy transfer pathway and quench the fluorescence of TPE in polymers. Consequently, the fluorescence of the poly (MMA-co-SPO-co-TPE) nanoparticles can be reversibly switched "on" and "off" upon UV and visible light, which maybe have potential application in biological fluorescent labeling as well as in optical fields like individually light–addressable nanoscale devices.

Keywords: *spirooxazine dye; photochromism; polymeric nanoparticles; aggregation-induced emission; tetraphenylethylene derivative.*

1. Introduction

Photochromic compounds display a reversible molecular structure transformation, which result in significant absorption spectra change upon the stimulation of ultraviolet (UV) and visible light.[1, 2] The special optical property makes them have high potential application in optical data storage, chemical sensors, optical switches, ophthalmic lenses, security documents.[3-7] Among a broad variety of photochromic compounds, spirooxazines have received considerable attention because of their fast response speed and good fatigue resistant.[8-10]

Photochromic molecules can be engineered to control the emission of fluorephore-photochrome dyads by energy transefer that caused by reversible photoinduced transformation.[11-18] So far, a number of photoswitchable fluorescent polymers containing spirooxazine have been reported[19-23] and their development have been extended micrometer/nanometersized level.[24] Photoswitchable fluorescent nanoparticles (PFNs) has been widely studied because of their potential biological application, such as ultrahigh-resolution imaging,[25] two photon imaging.[26] Many strategies have been developed to prepare PFNs, such as precipitation, self-assemble method, and emulsion polymerization. However, the self-assembly strategy maybe involves a complicated synthesis and the precipitation strategy often obtained PFNs via doping fluorescence dyes with photochromic molecules or polymer, which will lead to the leakage and aggregation of dyes over time.[27-29] In order to overcome these defects, semi-continuous emulsion polymerization, a facile and simple route was adopted.

Photoswitchable fluororescent materials are often utilized in their solid states, however, most of the luminophores will lead to aggregation-caused quenching (ACQ). Fortunately, Tang group[30] firstly discovered a new type of fluorescent molecular with Aggregation-induced emission. The AIE effect is opposite to the ACQ effect,[31] which makes it more valuable in practical application. In fact, the studies of polymers exhibit photochromic fluorescent properties and AIE properties are rarely reported.

Here, we utilized photochromic molecules spirooxazine (SPO) derivative and the typical AIE molecule tetraphenylethylene (TPE) derivative to prepare a series of polymeric nanoparticles with AIE and photochromic properties via semi-continuous emulsion polymerization. The fluorescence of the polymer nanoparticle can be switched “on” and “off” with UV and visible light.

2.Experimental

2.1 Materials and instruments

Potassium persulfate (KPS, 99%, Aladdin) was recrystallized from deionized water three times and dried under vacuum. Methyl methacrylate (MMA, 99.5%, Aladdin) was washed five times with 5% sodium hydroxide solution to remove the phenolic inhibitor and then washed with deionized water until the pH was 7. In addition, it was further purified upon distillation under reduced pressure and keep refrigerated for later experiment. Methylated-β-cyclodextrin, bromotriphenylethylene, 2-bromoethanol, methacryloylchloride, tetrabutylammonium bromide, tetrakis (triphenylphosphine) palladium (0) were purchased from Aladdin company. 2, 7-dihydroxynaphthalen, 1，3，3-trimethyl-2-methyleneindoline, 4-formylphenylboromic, allyl cyanoacetate were purchased from TCI company. Tetrahydrofuran (THF, A.R) was distilled over CaH_2. Deionized water was used for all experiments. Other solvents were analytical pure and without any further drying or purification.

Molecular weight of the polymers were obtained by using gel permeation chromatography (GPC). ^{1}H NMR spectra were obtained by a Bruker Avance 400 NMR spectrometer；UV-Vis spectra were carried out on Agilent 8453 UV-visible spectroscopy system；Fluorescence spectra were measured by Agilent Cary Eclipse Fluorescence Spectrophotometer. The polymeric nanoparticles diameter distribution and morphology was determined by Zetasizer Nano-ZS MPT and Hitachi S-4800 scanning electron microscope (SEM).

2.2 Synthesis of compound **4**:

Intermediate **3** was prepared according to the literature procedure,[32] the preparation method of spirooxazine derivative **4** was follow: adding **3** (1.07 g, 3.1 mmol), anhydrous K_2CO_3 (1.28 g, 9.3 mmol), 2-bromoethyl methacrylate (1.8 g, 9.3 mmol) and KI (0.515 g, 3.1 mmol) in 50 mL DMF, and the mixture was stirred for 48h at 85 ^oC. Then dropping them into ice water and filtered. The precipitate was dissolved into ethyl acetate and washed with water three times. The organic phase was dried over anhydrous magnesium sulfate. The purified product was obtained by column chromatography with petroleum ether/ethyl acetate (v/v=10/1) as eluent, white solid (0.6 g, 42% yield). ^{1}H NMR (400 MHz, $CDCl_3$) δ 7.93 (s, 1H), 7.75 (s, 1H), 7.68 (d, J = 8.9 Hz, 1H), 7.61 (d, J = 8.7, 1H), 7.32-7.21 (m, 1H), 7.11 (t, J = 7.1

Hz, 2H), 6.99-6.84 (m, 2H), 6.61 (d, *J* = 7.7 Hz, 1H), 6.22 (s, 1H), 5.63 (s, 1H), 4.63 (t, *J* = 4.7 Hz, 2H), 4.49 (t, *J* = 4.7 Hz, 2H), 2.80 (s, 3H), 2.01 (s, 3H), 1.39 (t, *J* = 3.6 Hz, 6H). ^{13}C NMR (101 MHz, CDCl3) δ 167.39, 157.88, 150.35, 147.62, 144.91, 136.05, 135.88, 132.28, 129.97, 129.58, 128.04, 126.10, 124.81, 122.41, 121.51, 119.86, 117.10, 114.30, 107.15, 100.68, 98.59, 66.00, 63.16, 51.81, 29.66, 25.47, 20.82, 18.38.

2.3 Synthesis of compound **6**

2.3.1 Synthesis of 4-(1, 2, 2-triphenylvinyl)benzaldehyde **5**

Bromotriphenylethylene (3.35 g, 0.01 mol), 4-formylphenylboronicacid (2.25 g, 0.015 mol), 60mL toluene, anhydrous K_2CO_3 (4.9 8g, 0.036 mol), TBAB (0.3 g, 0.01 mol) were added to 100mL three-necked, round-bottomed flask in order. The mixtrue stirred at room temperature under nitrogen atmosphere for 30min. Then, $Pd(pph_3)_4$ was added to the flask and the solution was heated to 90°C over 24h. The mixture solution was extracted with dichloromethane and the extract was dried with anhydrous magnesium sulfate. Further purification was accomplished by silica gel column chromatography with petroleum ether/ethyl acetate (v/v=20/1) as eluent, yellow solid (3.16 g, 87.8% yield).

2.3.2 Synthesis of allyl 2-cyano-3-(4-(1, 2, 2-triphenylvinyl) acrylate **6**

5 (1.08 g, 3 mmol), allylcyanoacetate (1.13 g, 9 mmol), NH_4OH (0.7 g, 9 mmol), ACOH 15mL were reflux for 24h in 50mL of toluene. The mixture solution was extracted with dichloromethane and the extract was washed three times with water, than dried with anhydrous magnesium sulfate. The purified product was obtained by column chromatography with petroleum ether/ethyl acetate (v/v=30/1) as eluent, yellow solid (2 g, 90% yield). ^{1}H NMR (400 MHz, $CDCl_3$) δ 8.17 (s, 1H), 7.78 (d, *J* = 8.2 Hz, 2H), 7.17 (dd, *J* = 9.3, 5.4 Hz, 12H), 7.06 (d, *J* = 7.1 Hz, 6H), 6.01 (m, *J* = 16.4, 10.8, 5.6 Hz, 1H), 5.45 (d, *J* = 17.1 Hz, 1H), 5.34 (d, *J* = 10.4 Hz, 1H), 4.82 (d, *J* = 5.5 Hz, 2H). ^{13}C NMR (101 MHz, CDCl3) δ 162.46, 154.86, 149.82, 143.40, 143.02, 142.95, 142.81, 139.62, 132.22, 131.39, 131.33, 131.30, 131.25, 131.13, 130.75, 129.32, 128.01, 127.99, 127.74, 127.23, 126.94, 119.19, 115.64, 101.42, 66.90.

2.4 Preparation of the poly (MMA-co-SPO-co-TPE) nanoparticles:

10mL water and methylated β-cyclodextrin (β-CD) was added into 50mL flask equipped with magnetic stirring bars. The solution was heated to 80℃ and deaerated by bubbling with nitrogen for 10min.Then KPS was added and the solution was heated under stirring for 30min. The spirooxazine compound **4** (SPO), tetraphenylethylene (TPE) compound **6** were dissolved in MMA and added dropwise via syringes over a period of 2h to the stirred solution at 80℃. After the addition of the monomers were completed, the reaction solution were heated at 85℃ for another five hours.

Scheme.1

Table.1

Fig.1

3. Result and discussion:

3.1 Synthesis

The synthetic route of the monomers spirooxazine compound **4** (SPO), tetraphenylethylene (TPE) compound **6** were presented in Scheme.1, and the preparation of polymer nanoparticles was shown in Fig. 1. The copolymers were consisted of three parts: photochrome, fluorogen and connection chains MMA, all the chemicals and their amounts were listed in Table 1. Among them, the photochrome act as energy receptor and the fluorogen act as energy donor, thereby the fluorescence of the polymer can be modulated by the energy transfer. In order to synthesize photochromic polymeric nanoparticles, we firstly prepared the photochromic spirooxazine nanoparticles with aggregation-induced emission by semi-continuous emulsion polymerization. In this preparation, MMA, TPE 6 and SPO 4 act as copolymerization monomers, KPS act as the initiator, β-CD is a ring moleculer consisting of a hydrophobic cavity and hydrophilic out side. This structure made it be able to form host-guest compounds with hydrophobic molecules, the formation complexs will increase the solubility of guest moleculer in aquese solution considerably.[33, 34] When the monomers were added to the β-CD aqueous solution semicontinuously, the concentration ratio of β-CD/monomers was kept in a high level, which enables fast complexation, and the complexes would become polymerizationsites. The β-CD plays an important role in increasing the rates of monomers conversation and polymerization in emulsion polymerization. In addition, due to the presence of β-CD in all steps only homogeneous nucleation occurs, which was contributes to the formation of stable uniform colloidal particles with a narrow

PSD.[35, 36] The structures of products were confirmed by NMR, IR spectroscopy and mass spectrometry.

3.2 Size and morphological of the poly (MMA-co-SPO-co-TPE) nanoparticles

Paticle size and size distribution of **P1** to **P4** were obtained by dynamic light scattering (DLS) analysis and shown in Fig. 2. Their size increased from 355 nm to 657 nm with the increased in SPO monomer ratio. Morphology was determined by scanning electron microscopy and displayed in Fig. 3. The results indicated that all the samples were smooth and uniform. Fig. 4a and Fig.4b showed the images of **P2** under general microscope and fluorescence microscope, respectively. The fluorescent photo illustrated that the AIE fluorophore was incorporated to the nanoparticles successfully. We can believe that the semi-continous emulsion polymerization is an appropriate method to preparation nanoparticle polymer.

Fig.2

Fig.3

Fig.4

3.3 Thermal properties of the poly (MMA-co-SPO-co-TPE) nanoparticles

Thermal properties of the four polymers were evaluated by thermogravimetric analysis (TGA). The decomposition temperature (T_d) of these polymers (corresponding to 5% weight loss occurs during heating in nitrogen) were 284.7□, 287.02□, 276.05□, 280.72□, respectively (Fig. 5). The results indicate that the polymers have a relatively high thermal stability, to the best of our knowledge, a relatively high T_d is crucial for emissive materials used for optoelectronic applications.

Hence, the synthesized polymers might be used as potential meterials for applications in fabricated photoelectric devices.

Fig.5

3.4 Photochromism of spirooxazine 4 and AIE properties of the compound 6

Fig. 6 showed the absorption spectra and color change of spirooxazine (SPO) 4 in DMF (2.0×10^{-5} mol L^{-1}) irradiation with UV and visible light. Before irradiation with UV light, the spirooxazine (SPO) 4 in DMF solution was colorless and has no absorbance at about 600 nm. By UV irradiation (365 nm), the sample become blue and with an increased absorbance intensity at 602 nm, when it was left in the dark or irradiated with visible light at ambient temperature, the color was fading and the absorbance was decreased again. The reason is that the structure of spirooxazine (SPO) 4 change from orthogonal closed cycle to opened merocyanine form. The opened form is usually thermally unstable and spontaneously underwent thermal bleaching to the close cycle form.

The corresponding emission spectra of the compound 6 in water/DMF mixtures with different water fraction (f_w) are shown in Fig. 7a. As can be seen from the figure, the PL signals of compound 6 in a dilute solution of DMF almost couldn’t be detected and the luminescence intensity almost unchanged when f_w was increased to 60%. However, a dramatic enhancement in luminescence was occured when f_w was beyond 60%, and it boosted to 530.7 a.u. at the water fraction of 90% while the highest PL intensity value was measured only about 3.1 a.u. in pure DMF, the maximum increase in the emission intensity is~170-fold. Because there is not so solvable for compound

6 in water, the molecular become aggeregation formation in the mixtures with higher water content. Hence, the PL intensity was enhanced remarkably by restricted intramolecular rotations (RIR) process in the crowed invironment. The absorption spectra of compound 6 in the DMF/water mixtures were shown in Fig. 7b. The spectra were significant changed when water fraction was up to 70% or higher. Fig. 7c showed the images of the compound 6 were taken under room light (top) and 365 nm UV light (bottom) at room temperature in DMF/water mixtures with different water fractions.

Fig.6

Fig.7

3.5 Photochromic properties of the poly (MMA-co-SPO-co-TPE) nanoparticles

The spectra changes of polymers (**P1**, **P2**, **P3**, **P4**) in DMF solution (2.5mg/mL) upon UV and visible light irradiation were shown in Fig. 8. With the irradiation of UV light (365 nm) at room temperature, a new absorption band with λ_{max}= 605 nm was observed and the solution was changed from colorless to blue, corresponding to the generation of the opened merocyanine form in SPO units. In addition, these studies also revealed that the absorption intensity increased with the increase of SPO/TPE ratio. Fig.9a showed the changes in the absorption spectra of **P2** in an aqueous suspension before and after UV illumination. The absorbance band occurs at 525 to 675 nm upon UV irradiation, The inset figure showed the color change of **P2** latex, with the irradiation of UV light the latex was turned to blue from milk white. The absorption spectra change of **P2** in film was shown in Fig. 9b. The reversible bleaching process of film was similar to that in the DMF solution. After the irradiation of UV light an absorption peak appeared at 605 nm, then the peak disappeared upon the irradiation of the visible light. The polymer film has excellent photochromic fatigue resistance. Because of the steric effects in solid powder, the photochromic stability of the polymer powder was enhanced significantly than that of in DMF solution. The inset figure showed the color change of **P2** in solid powder.

Fig.8

Fig.9

3.6 AIE Properties of the poly (MMA-co-SPO-co-TPE) nanoparticles

We detected the fluorescent emission of all the polymers in a mixture of water and DMF with different water fractions, and the corresponding emission spectra of **P1** and **P2** are shown in Fig. 10. The fluorescence intensity change of **P1** with the increasingin water fraction was very different from the monomer TPE, when f_w was increased to 20%, the PL intensity of the solutions stared increase obviously (Fig. 10a). The possible reason was that polymer chains were more hydrophobic and have a higher tendency to aggregate in a polar medium when compared with the monomer molecules. So the light emission of **P1** significantly enhanced in water fraction as low as 20% by aggregate formation. The emission intensity reached a maximum with water fraction upto 30%, then PL intensities decreased with higher water content. As can be seen from Fig. 10b, when f_w varies from 0% to 70%, the PL intensity of **P2** increase gradually, however the f_w is increased to 80% or higher, the PL intensity decreases with increasing water content. This phenomenon was often observed in some compounds with AIE properties, but the reasons remain unclear.[37] There are two possible explanations for this phenomenon: First, according to the aggregation with the increasing of the water fraction in solvent, only the molecules on the surface of the nanoparticles emitted light and contributed to the fluorescent intensity upon excitation, leading to the decrease of the fluorescent intensity; but the restriction of intramolecular rotations (RIR) of the aromatic rings aroundthe carbon-carbon single bonds in the aggregation state would enhance light emission. The net outcome of these two antagonistic processes depends on which process plays a predominant role in affecting the fluorescent behavior of the aggregated molecules. Second, when water is added, the solute molecules may aggregate into crystal and amorphous particles. The former leads to an enhancement in the intensity of photoluminescent emission, while the latter leads to its reduction. Thus, the measured photoluminescent intensity often shows no regularity for the uncontrollable formation of the nanoparticles in solutions with high water content.[38-48]

The inset in Fig. 10 showed that the maximum emission wavelength changes and fluorescence intensity changes with increasing water fraction, the maximum emission wavelength had a blue shift. Fluorescence emission spectra of **P3** in DMF-H_2O mixture with different f_w were demonstrated in the Fig. S9, nearly the same trends were observed in the case of **P3**, however, the maximum PL intensity is weaker than **P1** and **P2**. Almost no fluorescence signal was detected for **P4** no matter in pure DMF solution or in water/DMF mixtures. The weaker emission was ascrible the low content of TPECN unit in **P3** or **P4**. UV absorption spectra of all the polymers with different water fraction were displayed in Fig. S10, they all showed a long-wavelength absorption tail caused by light-scattering effects in the solution. Fig. 11 showed the images of the **P1** and **P2** were taken under room light (top) and 365 nm UV light (bottom) at room temperature in DMF/water mixtures with different water fractions.

Fig.10

Fig.11

3.7 Photocontrolled fluorescence properties of the poly (MMA-co-SPO-co-TPE) nanoparticles

The fluorescence intensity changes of the **P1** and **P2** in DMF-H_2O mixture solution were described in Fig. 12a and Fig. 12b. The two figures indicated that fluorescence intensity changes were regulated with the irradiation of UV and visible light both of P1 and P2. The fluorescence quenching rate of **P1** was only about 56% and the fluorescence quenching rate of **P2** was about 70% upon irradiation with UV, which instructed that the fluorescence quenching rate of the polymer may be adjusted by changing the ratio of SPO and TPE in polymer. After irradiation with visible light, the fluorescence intensity gradually recovered to the original intensity, and this process can be recycled many times, which has vast potential application for photochromic fluorescence switch. Fig. 12c and Fig. 12d showed the fluorescence intensity changes of **P1** and **P2** in film, the case of fluorescence quenching were similar to that of in DMF-H_2O mixture solution.

The absorption of the opened merocyanine form was from 400 nm to 700 nm and the emission band of fluorophore unit was from 450 nm to 600 nm, that is to say, their spectra exists overlap in the range of 450 nm to 600 nm. Therefore, when the SPO unit of the polymer from closed form to merocyanine with the irradiation of UV, it will absorb the emitted light of TPE because of the energy transfer resulting in the fluorescence quenching of the polymer. With the irradiation of visible light the merocyanine return to closed cycle form, there is no overlap of the absorption spectrum and the emission spectrum, the fluorescence intensity recover.

Fig.12

4. Conclusions

In conclusion, four polymeric nanoparticles with spirooxazine derivative and AIE fluorescent dye were synthesized by semi-continuous polymerization. All the nanopartice polymers are uniform and display a narrow particle size distribution. Their photochromic properties and AIE properties have been studied detailedly, showing that all the polymers exhibit excellent photochromic ability. **P1** and **P2** exhibit good AIE properties and their fluorescence intensities could be modulated regularly with irradiation of UV and visible light. Thus indicates that **P1** and **P2** may be potential candidate for external stimuli-responsive materials, such as photoswitch, bioprobe and so on.

Acknowledgements

This work was financially supported by NSFC (21372194，20802065 and 21476075), and the GuangGong Yangfan Talent Plan (2013).

References

[1] Irie M. Photochromism: Memories and switches introduction. Chem Rev 2000;100(5):1683-4.

[2] Irie M, Fukaminato T, Matsuda K, Kobatake S. Photochromism of diarylethene molecules and crystals: memories, switches, and actuators. Chem Rev 2014;114(24):12174-277.

[3] Bertarelli C, Bianco A, Castagna R, Pariani G. Photochromism into optics: opportunities to develop light-triggered optical elements. J Photochem Photobiol C: Photochem Rev 2011;12(2):106-25.

[4] De Silva AP, Gunaratne HQN, Gunnlaugsson T, Huxley AJM, Mccoy CP, Rademacher JT, et al. Signaling recognition events with fluorescent sensors and switches. Chem Rev 1997;97(5):1515-66.

[5] Feczkó T, Samu K, Wenzel K, Neral B, Voncina B. Textiles screen-printed with photochromic ethyl cellulose-spirooxazine composite nanoparticles. Color Technol 2013;129(1):18-23.

[6] Sriprom W, Neel M, Gabbutt CD, Heron BM, Perrier S. Tuning the color switching of naphthopyrans via the control of polymeric architectures. J Mater Chem 2007;17(19):1885-93.

[7] Zhao W, Carreira EM. A smart photochromophore through synergistic coupling of photochromic subunits. J Am Chem Soc 2002;124(8):1582-3.

[8] Chu NYC. Photochromism of spiroindolinonaphthoxazine. I. photophysical properties. Can J Chem 1983;61:300-305.

[9] Chu NYC. Photochromic Performance of Spiroindolino-naphthoxazines in Plastics. Solar Energy Materials. 1986;14:215-221.

[10] Malatesta GR V, Romano U, Allegrini. P. Photochromic spironaphthoxazines: a theoretical study. Int J quantum chem 1992;42:879-87.

[11] Cusido J, Ragab SS, Thapaliya ER, Swaminathan S, Garcia-Amorós J, Roberti MJ, et al. A photochromic bioconjugate with photoactivatable fluorescence for superresolution imaging. J Phys Chem C 2016;120(23):12860-70.

[12] Fukaminato T. Single-molecule fluorescence photoswitching: Design and synthesis of photoswitchable fluorescent molecules. J Photochem Photobiol C: Photochem Rev 2011;12(3):177-208.

[13] Giordano L, Jovin TM, Irie M, Jares-Erijman EA. Diheteroarylethenes as thermally stable photoswitchable acceptors in photochromic fluorescence resonance energy transfer (pcFRET). J Am Chem Soc 2002;124(25):7481-9.

[14] Kim S, Yoon S-J, Park SY. highly fluorescent chameleon nanoparticles and polymer films: multicomponent organic systems that combine FRET and photochromic switching. J Am Chem Soc 2012;134(29):12091-7.

[15] Yang Z, Cao J, He Y, Yang JH, Kim T, Peng X, et al. Macro-/micro-environment-sensitive chemosensing and biological imaging. Chem Soc Rev 2014;43(13):4563-601.

[16] Yildiz I, Impellizzeri S, Deniz E, McCaughan B, Callan JF, Raymo FM. Supramolecular strategies to construct biocompatible and photoswitchable fluorescent assemblies. J Am Chem Soc 2011;133(4):871-9.

[17] Yun C, You J, Kim J, Huh J, Kim E. Photochromic fluorescence switching from diarylethenes and its applications. J Photochem and Photobiol C: Photochem Rev 2009;10(3):111-29.

[18] Zhou X, Wu X, Yoon J, A dual FRET based fluorescent probe as a multiple logic system. Chem Commun 2015;51(1):111-3.

[19] Kim S-H, Hwang I-J, Gwon S-Y, Son Y-A. Photoregulated optical switching of poly(N-isopropylacrylamide) hydrogel in aqueous solution with covalently attached spironaphthoxazine and D-π-A type pyran-based fluorescent dye. Dyes Pigm 2010;87(2):158-63.

[20] Lee EM, Gwon SY, Ji BC, Wang S, Kim SH. Multiple switching behaviors of poly(N-isopropylacrylamide) hydrogel with spironaphthoxazine and D-π-A type dye. J Lumi 2012;132(3):665-70.

[21] Lee EM, Gwon SY, Son YA, Kim SH. Switching properties of fluorescent photochromic poly(methyl methacrylate) with spironaphthoxazine and D-π-A type pyran-based fluorescent dye. Spectrochim Acta A 2012;86:600-4.

[22] Wang S, Yu C, Choi M, Kim S. A switching fluorescent photochromic carbazole–spironaphthoxazine copolymer. Dyes Pigm 2008;77(1):245-8.

[23] Wang S, Yu C, Choi M-S, Kim S-H. Synthesis and switching properties of photochromic carbazole–spironaphthoxazine copolymer. J Photochem Photobiol A: Chem 2007;192(1):17-22.

[24] Elizabeth J. Harbron CMD, Joshua K. Campbell, Rebecca M. Allred, Marissa T. Kovary, and Nicholas J. Economou. Photochromic dye-doped conjugated polymer

nanoparticles: photomodulated emission and nanoenvironmental characterization. J Phys Chem C 2009;113:13707-14.

[25] Tian Z, Li ADQ. Photoswitching-enabled novel opticalimaging: innovative solutions for real-world challenges in fluorescence detections. Accounts Chem Res 2013;46(2):269-79.

[26] Zhu MQ, Zhang GF, Li C, Aldred MP, Chang E, Drezek RA, et al. Reversible two-photon photoswitching and two-photon imaging of immunofunctionalized nanoparticles targeted to cancer cells. J Am Chem Soc 2011;133(2):365-72.

[27] Abdollahi A, Mahdavian AR, Salehi-Mobarakeh H. Preparation of stimuli-responsive functionalized latex nanoparticles: the effect of spiropyran concentration on size and photochromic properties. Langmuir 2015;31(39):10672-82.

[28] Chen J, Zhong W, Tang Y, Wu Z, Li Y, Yi P, et al. Amphiphilic BODIPY-based photoswitchable fluorescent polymeric nanoparticles for rewritable patterning and dual-color cell imaging. Macromolecules 2015;48(11):3500-8.

[29] Harbron EJ. Photochromic nanoparticles. photochem. 2011;39:211-27.

[30] Luo J, Xie Z, Lam JWY, Cheng L, Chen H, Qiu C, et al. Aggregation-induced emission of 1-methyl-1,2,3,4,5-pentaphenylsilole. Chem Commun 2001(18):1740-1.

[31] Cui L, Beak Y, Lee S, Kwon N, Yoon J. An AIE and ESIPT based kinetically resolved fluorescent probe for biothiols. J Mater Chem C 2016;4(14):2909-14.

[32] Kim S-H, Choi S-W, Suh H-J, Jin S-H, Gal Y-S, Koh K. Surface plasmon resonance spectroscopy on the interaction of a self-assembled monolayer with linear hydrocarbon such as pentane, hexane, heptane and octane. Dyes Pigm

2002;55(1):17-25.

[33] Saenger W. Cyclodextrin inclusion compounds inresearch and industry. Angew Chem Int Ed 1980;19:344-62.

[34] Wenz G. Cyclodextrins as building blocks for supramolecular structures and functional units. Angew Chem In tEd 1994;33:803-22.

[35] Storsberg J, Van Aert H, Van Roost C, Ritter H. Cyclodextrins in polymer synthesis: a simple and surfactant free way to polymer particles having narrow particle size distribution. Macromolecules 2003;36(1):50-3.

[36] Heterz M, Schmidt BVKJ, Barner-Kowollik C, Ritter H. Limitations of cyclodextrin-mediated RAFT homopolymerization and back copolymer formation. J Poly Sci Part A: Poly Chem 2013;51(11):2504-17.

[37] Dong Y, Lam JWY, Qin A, Sun J, Liu J, Li Z, et al. Aggregation-induced and crystallization-enhanced emissions of 1,2-diphenyl-3,4-bis(diphenylmethylene)-1-cyclobutene. Chem Commun 2007;(31):3255-7.

[38] Li H, Chi Z, Zhang X, Xu B, Liu S, Zhang Y, et al. New thermally stable aggregation-induced emission enhancement compounds for non-doped red organic light-emitting diodes. Chem Commun 2011;47(40):11273.

[39] Qin A, Zhang Y, Han N, Mei J, Sun J, Fan W, et al. Preparation and self-assembly of amphiphilic polymer with aggregation-induced emission characteristics. Sci China Chem 2012;55(5):772-8.

[40] Dong S, Li Z, Qin. J. New Carbazole-Based Fluorophores: Synthesis,

Characterization, and aggregation-induced emission enhancement. J Phys Chem B 2009;113(2):434.

[41] Xu Bj, Chi ZG, Li XF, Li HY, Zhou W, Zhang XQ, et al. Synthesis and properties of diphenylcarbazole triphenylethylene derivatives with aggregation-induced emission, elue light emission and high thermal stability. J Fluoresc 2010;21(1):433-41.

[42] Zhang XQ, Chi ZG, Xu B, Li H, Yang Z, Li X, et al. Synthesis of blue light emitting bis(triphenylethylene) derivatives: A case of aggregation-induced emission enhancement. Dyes Pigm 2011;89(1):56-62.

[43] Chen M, Li L, Nie H, Tong J, Yan L, Xu B, et al. Tetraphenylpyrazine-based AIEgens: facile preparation and tunable light emission. Chem Sci. 2015;6(3):1932-7.

[44] He JT, Xu B, Chen FP, Xia HJ, Li KP, Ye L, Tian WJ. Aggregation-induced emission in the crystals of 9,10-distyrylanthracene derivatives: the essential role of restricted intramolecular torsion. J Phys Chem C 2009;113:9892–9.

[45] Liu C, He W, Shi G, Luo H, Zhang S, Chi Z. Synthesis and properties of a new class of aggregation-induced enhanced emission compounds: Intense blue light emitting triphenylethylene derivatives. Dyes Pigm 2015;112:154-61.

[46] Luo M, Wang S, Wang M, Huang S, Li C, Chen L, et al. Novel organogel harnessing excited-etate intramolecular proton transfer process with aggregation induced emission and photochromism. Dyes Pigm 2016;132:48-57.

[47] Yuan WZ, Zhao H, Shen XY, Mahtab F, Lam JWY, Sun JZ, et al. Luminogenic Polyacetylenes and conjugated polyelectrolytes: synthesis, hybridization with carbon nanotubes, aggregation-induced emission, superamplification in emission quenching

by explosives, and fluorescent assay for protein quantitation. Macromolecules 2009;42(24):9400-11.

[48] Xie ZQ, Yang B, Xie WJ, Liu LL, Shen FZ, Wang H, Yang XY, Wang ZM, Li YP, Muddasir H, Yang GD, Ye L, Ma YG. A class of nonplanar conjugated compounds with aggregation-induced emission: structural and optical properties of 2,5-diphenyl-1,4-distyrylbenzene derivatives with all cis double bonds. J Phys Chem B 2006;110:20993-21000.

Table 1. List of nanoparticles prepared with different ratio of SPO and TPE

polymer	SOMA (mmol)	TPECN (mmol)	MMA (mol)	RAMEB (mg)	water (g)	$K_2S_2O_8$ (mg)	D_m (nm)	M_n (g/mol)	PDI
P1	0.02	0.02	0.01	30	10	30	355.0	64714	2.86
P2	0.04	0.02	0.01	30	10	30	436.3	59441	2.04
P3	0.08	0.02	0.01	30	10	30	540.5	45864	1.75
P4	0.16	0.02	0.01	30	10	30	656.9	54291	2.03

Figure captions

Fig 1 Synthesis and photoswitchable process of polymer nanoparticles.

Fig 2 The size distribution of **P1**, **P2**, **P3** and **P4** by DLS at room temperature.

Fig 3 SEM images of **P1**, **P2**, **P3** and **P4**.

Fig 4 The image of **P2** under general microscope (a) and fluorescence microscope (b).

Fig 5 TGA curves of the polymers.

Fig 6 Absorption spectrum and color changes of SPO 6 in DMF solution（2.0×10^{-5} mol L^{-1}） upon irradiation with UV and visible light.

Fig 7 (a) PL spectra changes and (b) absorption spectra changes of TPE 6 in DMF/water mixtures with different water fractions. Concentration : 2×10^{-5}mol/L, λ_{ex} = 374 nm. (inset: the dependence of the fluorescence emission intensity on the water fraction). (c) the images of TPE in DMF/water mixtures with different water fractions were taken under room light (top) and 365 nm UV light (bottom).

Fig 8 Absorption spectra changes of polymers in DMF solution (2.5 mg/mL) before and after UV (365 nm) illumination. (a):**P1**; (b):**P2**; (c):**P3**; (d):**P4**.

Fig 9 Absorption spectra changes of **P2** (a) in an aqueous suspension and **P2** (b) in film before and after UV illumination. (inset: picture of P2 latexes and P2 solid before and after UV irradiation at 365 nm).

Fig 10 PL spectra change of (a) **P1** and (b) **P2** in water/DMF mixtures. The inset depicts the changes of PL peak intensity and maximum PL emission wavelength (0.5mg/mL).

Fig 11 the images of **P1** (a) and **P2** (b) in DMF/water mixtures with different water fractions were taken under room light (top) and 365 nm UV light (bottom).

Fig 12 PLspectra change of (a) **P1** in water/DMF mixtures with a water fraction of 30% (0.5mg/ml) and (b) **P2** in water/DMF mixtures with a water fraction of 80% (0.5mg/ml) upon irradiation with UV and visible light (λ_{ex}=302nm). PL spectra change of (c) **P1** in film and (d) **P2** in film upon irradiation with UV and visible light (λ_{ex}=302nm).

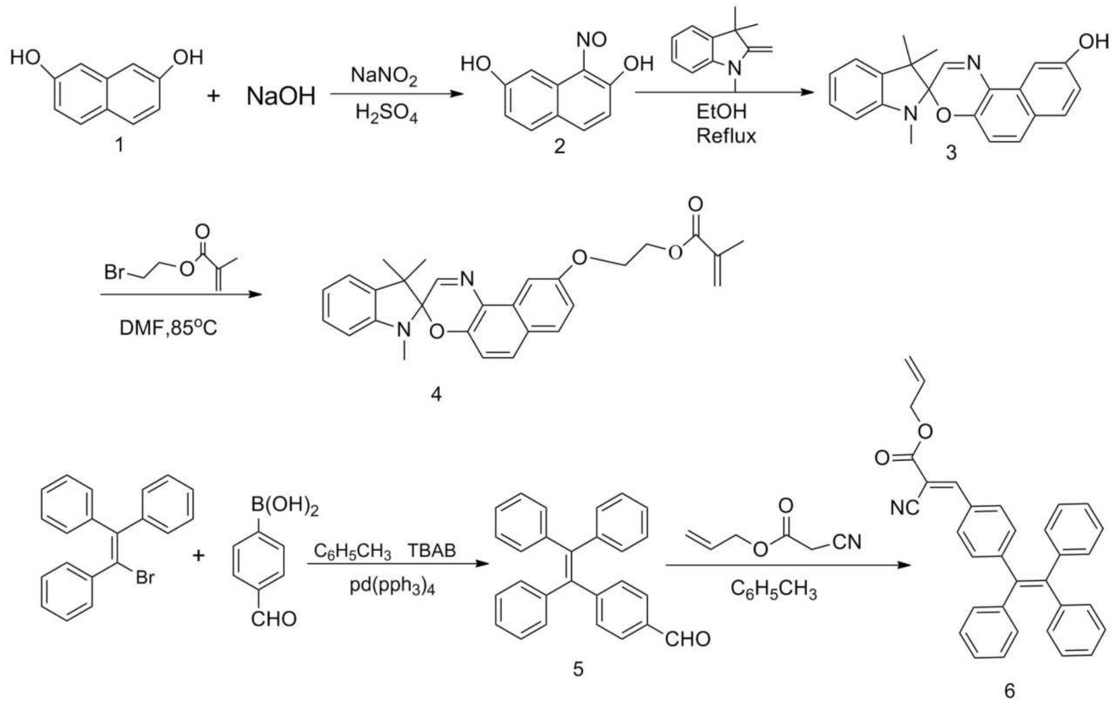

Scheme 1

Scheme 1 Synthetic routes for SPO 4 and TPE 6

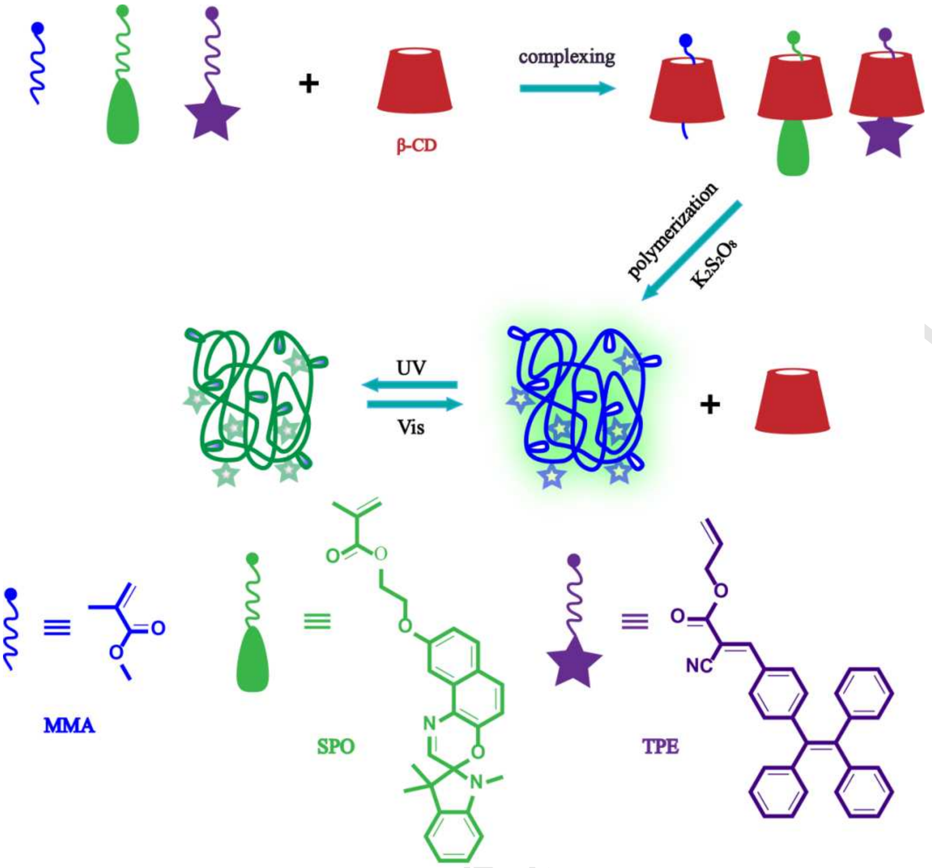
complexing
β-CD
polymerization
$K_2S_2O_8$
UV
Vis
MMA
SPO
TPE
O
O
O
N
O
N
O
O
O
NC

Fig. 1

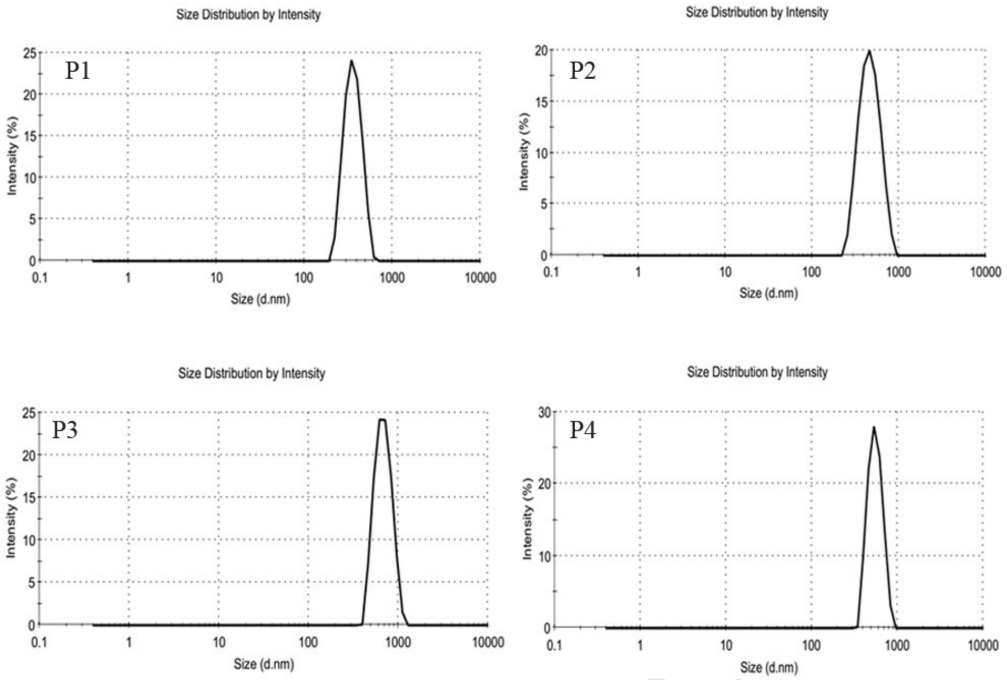
Size Distribution by Intensity
P1
Intensity (%)
0
5
10
15
20
25
Size (d.nm)
0.1
1
10
100
1000
10000
Size Distribution by Intensity
P2
Intensity (%)
0
5
10
15
20
Size (d.nm)
0.1
1
10
100
1000
10000
Size Distribution by Intensity
P3
Intensity (%)
0
5
10
15
20
25
Size (d.nm)
0.1
1
10
100
1000
10000
Size Distribution by Intensity
P4
Intensity (%)
0
10
20
30
Size (d.nm)
0.1
1
10
100
1000
10000

Fig. 2

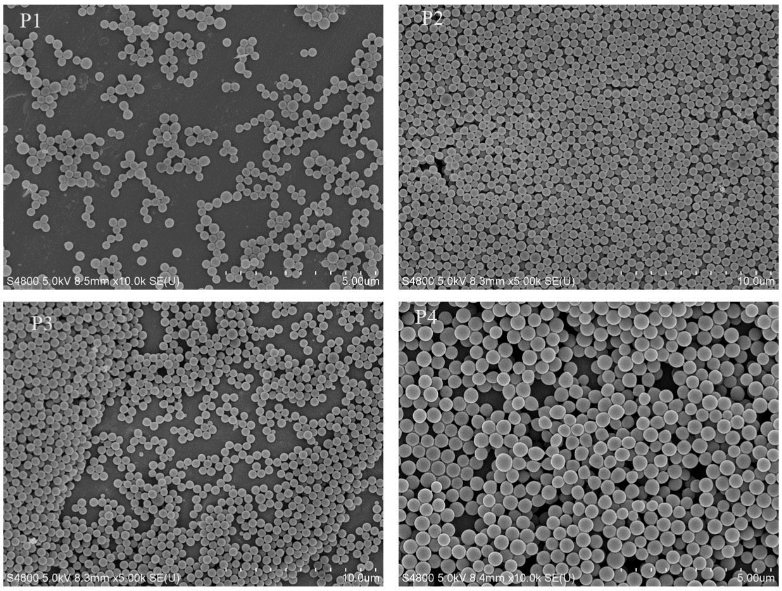
P1
S4800 5.0kV 8.5mm x10.0k SE(U)
5.00um
P2
S4800 5.0kV 8.3mm x5.00k SE(U)
10.0um
P3
S4800 5.0kV 8.3mm x5.00k SE(U)
10.0um
P4
S4800 5.0kV 8.4mm x10.0k SE(U)
5.00um

Fig. 3

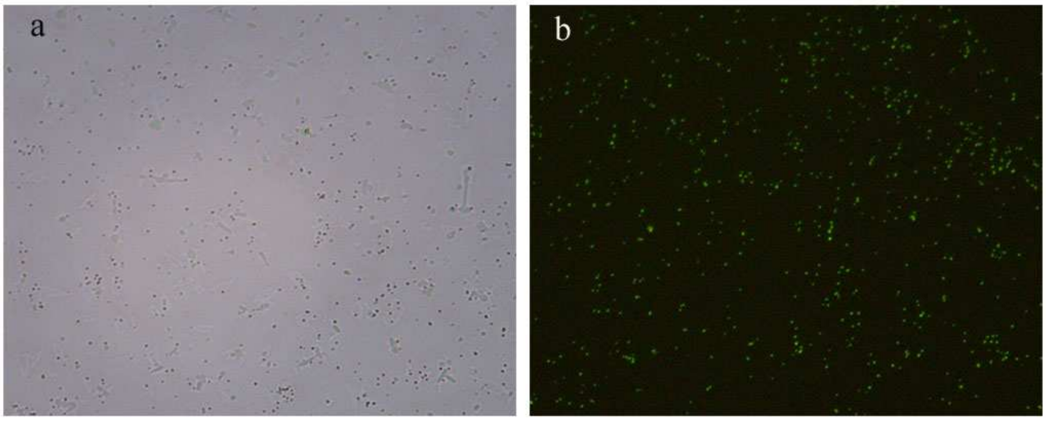

Fig. 4

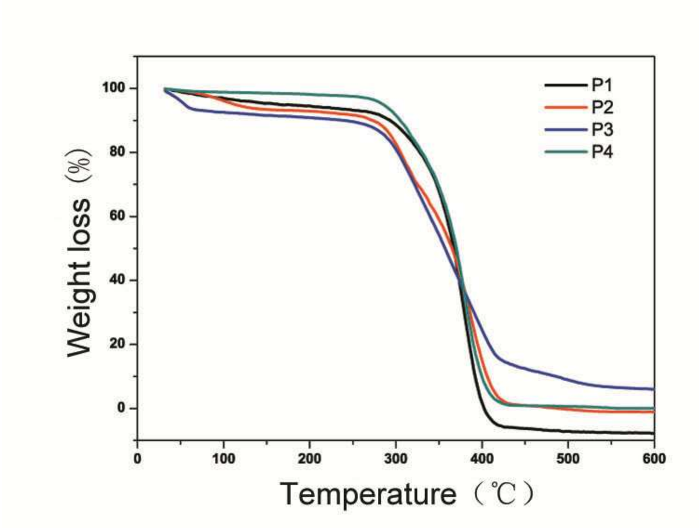
Weight loss (%)
Temperature（℃）
100
80
60
40
20
0
0
100
200
300
400
500
600
P1
P2
P3
P4

Fig. 5

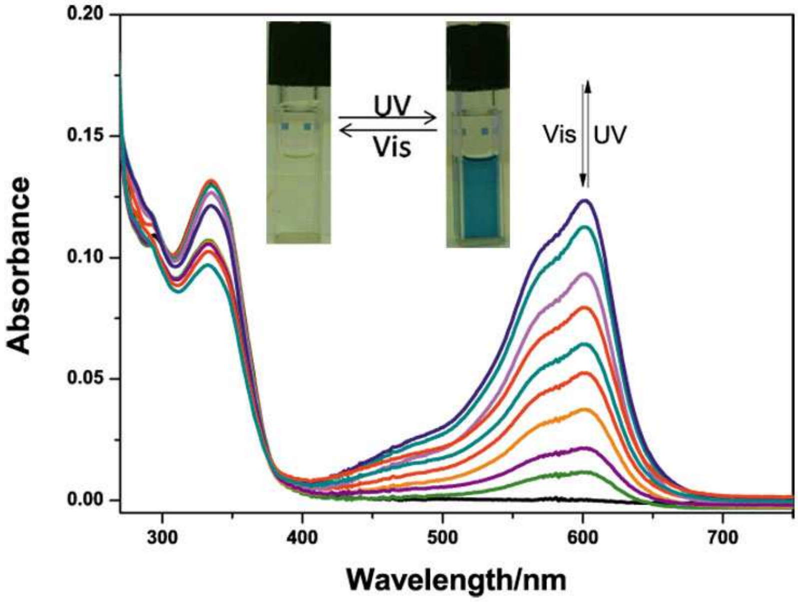
Absorbance
Wavelength/nm
0.20
0.15
0.10
0.05
0.00
300
400
500
600
700
UV
Vis
Vis
UV

Fig. 6

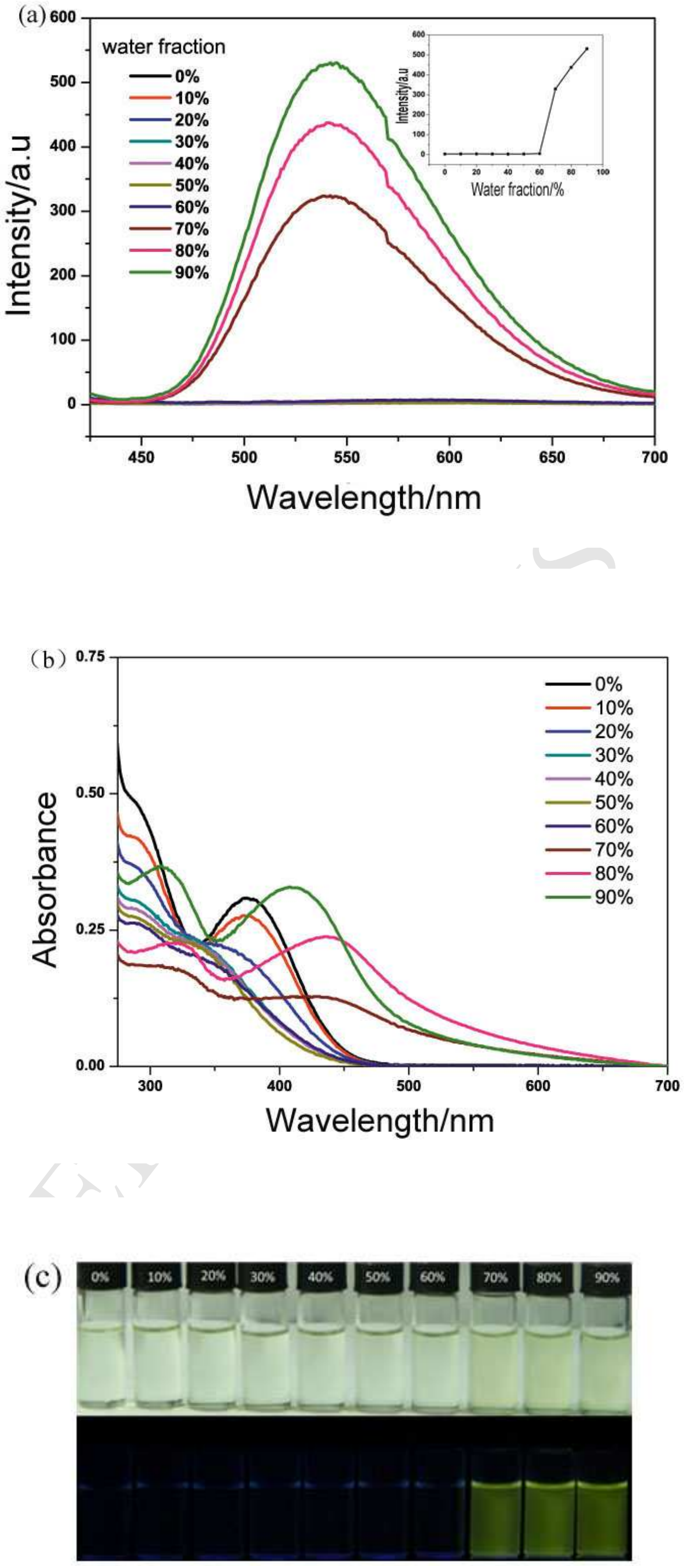
(a)
water fraction
0%
10%
20%
30%
40%
50%
60%
70%
80%
90%
Intensity/a.u
Wavelength/nm
Intensity/a.u
Water fraction/%
(b)
Absorbance
Wavelength/nm
0%
10%
20%
30%
40%
50%
60%
70%
80%
90%
(c)
0%
10%
20%
30%
40%
50%
60%
70%
80%
90%

Fig. 7

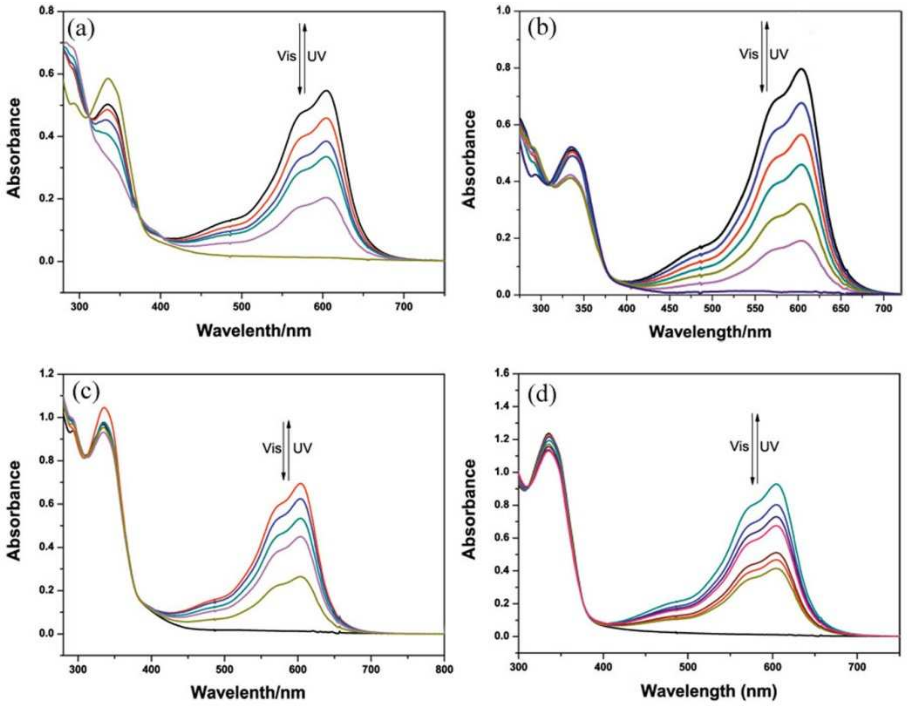
(a)
Vis
UV
Absorbance
Wavelenth/nm
0.8
0.6
0.4
0.2
0.0
300
400
500
600
700
(b)
Vis
UV
Absorbance
Wavelength/nm
1.0
0.8
0.6
0.4
0.2
0.0
300
350
400
450
500
550
600
650
700
(c)
Vis
UV
Absorbance
Wavelenth/nm
1.2
1.0
0.8
0.6
0.4
0.2
0.0
300
400
500
600
700
800
(d)
Vis
UV
Absorbance
Wavelength (nm)
1.6
1.4
1.2
1.0
0.8
0.6
0.4
0.2
0.0
300
400
500
600
700

Fig. 8

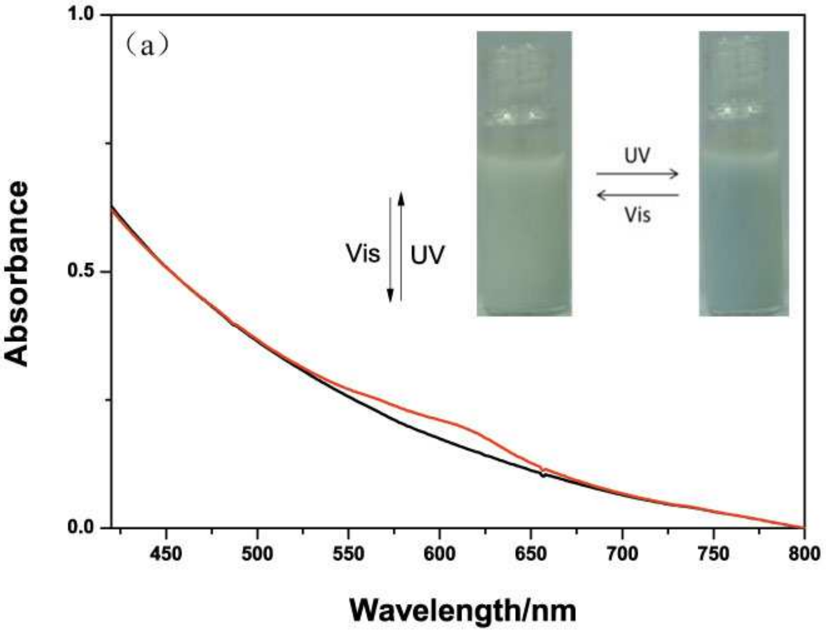
(a)
Absorbance
1.0
0.5
0.0
450
500
550
600
650
700
750
800
Wavelength/nm
Vis
UV
UV
Vis

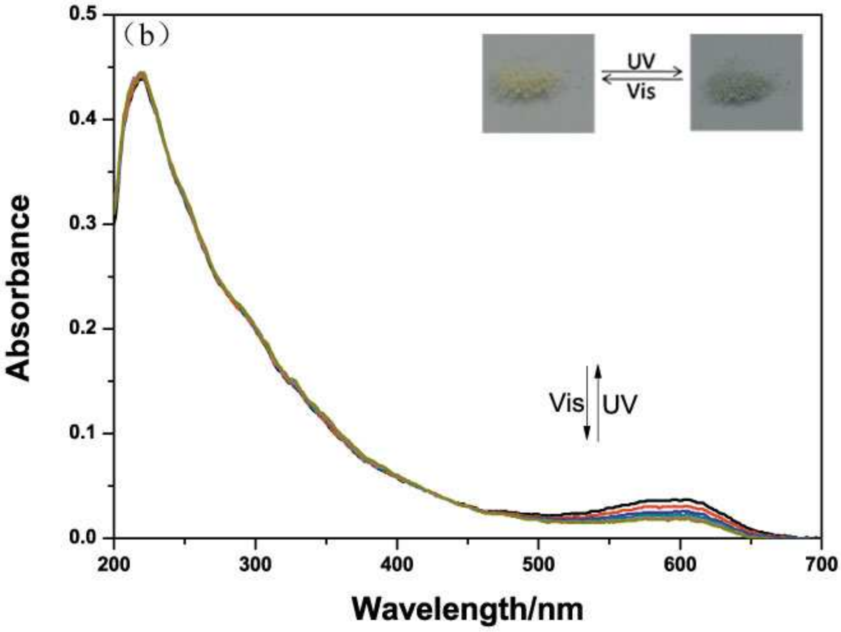
(b)
Absorbance
0.5
0.4
0.3
0.2
0.1
0.0
200
300
400
500
600
700
Wavelength/nm
UV
Vis
Vis
UV

Fig. 9

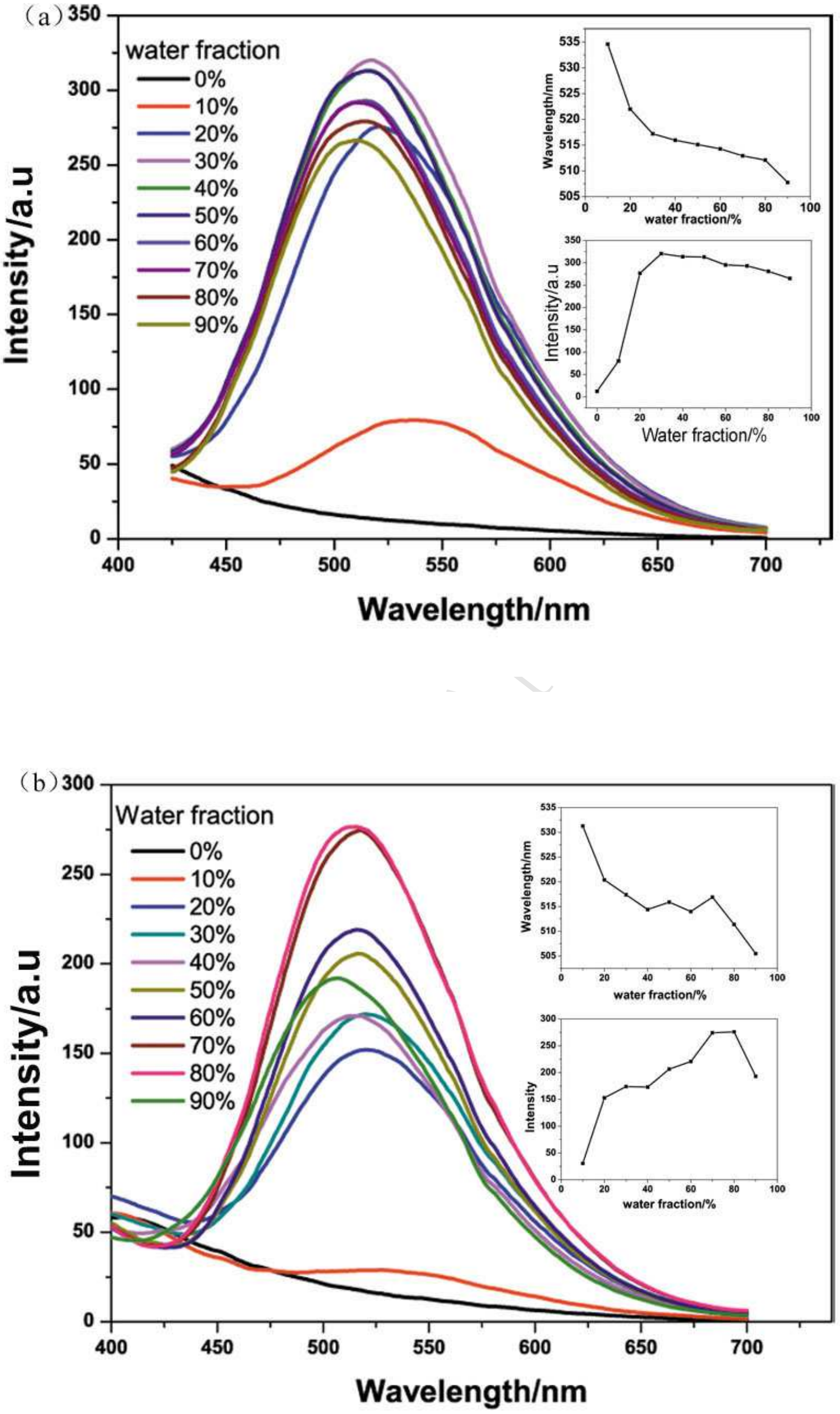
（a）
water fraction
0%
10%
20%
30%
40%
50%
60%
70%
80%
90%
Intensity/a.u
Wavelength/nm
0
50
100
150
200
250
300
350
400
450
500
550
600
650
700
Wavelength/nm
water fraction/%
Intensity/a.u
Water fraction/%
（b）
Water fraction
0%
10%
20%
30%
40%
50%
60%
70%
80%
90%
Intensity/a.u
Wavelength/nm
Wavelength/nm
water fraction/%
Intensity
water fraction/%

Fig. 10

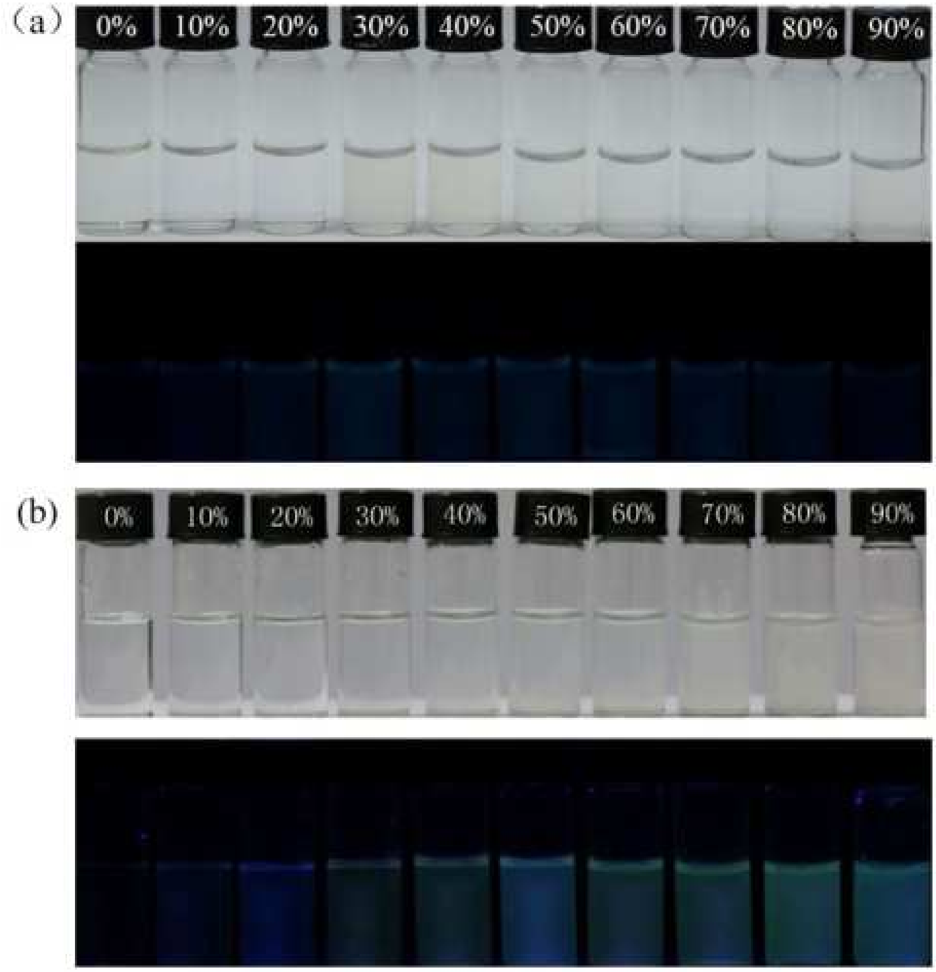

Fig. 11

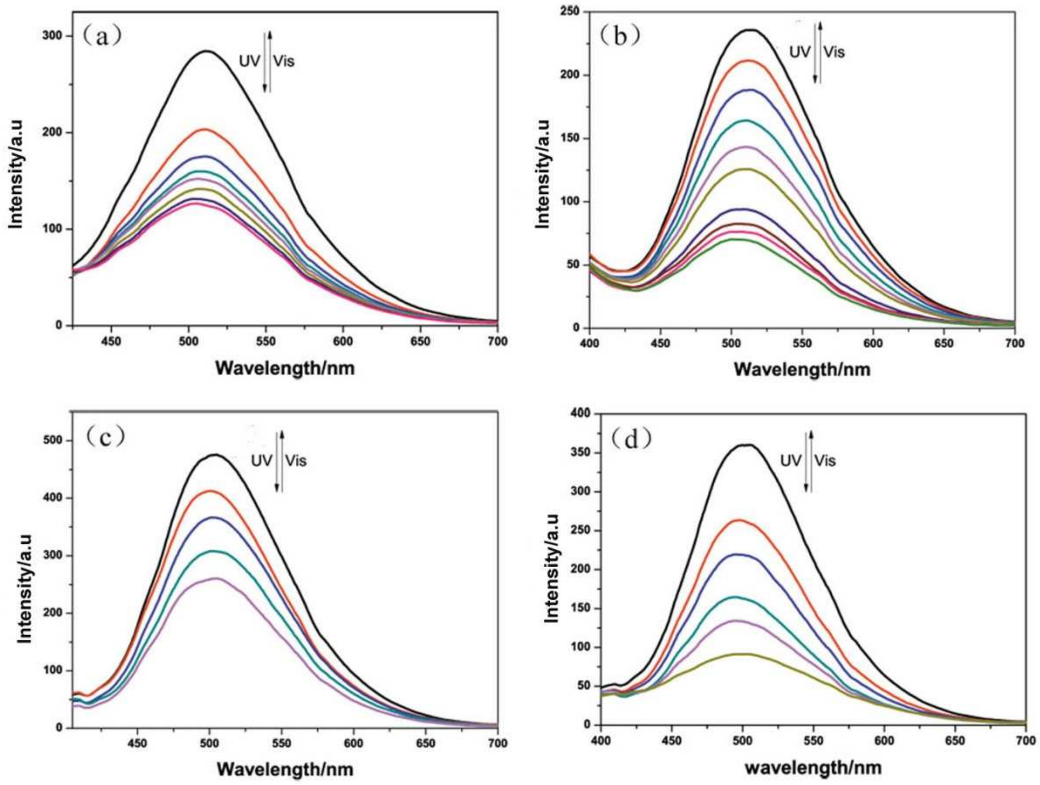
(a)
UV
Vis
Intensity/a.u
Wavelength/nm
0
100
200
300
450
500
550
600
650
700
(b)
UV
Vis
Intensity/a.u
Wavelength/nm
0
50
100
150
200
250
400
450
500
550
600
650
700
(c)
UV
Vis
Intensity/a.u
Wavelength/nm
0
100
200
300
400
500
450
500
550
600
650
700
(d)
UV
Vis
Intensity/a.u
wavelength/nm
0
50
100
150
200
250
300
350
400
400
450
500
550
600
650
700

Fig. 12

Supporting information

Synthesis and Properties of Photochromic Spirooxazine with Aggregation-Induce Emission Fluorophores polymeric nanoparticles via Semi-continuous Emulsion Polymerization

Xue Li[a,b], Chengpeng Li[b], Sheng Wang[a,b,]*, Huan Dong[c], Xiang Ma[c,]**, Derong Cao[a,]**

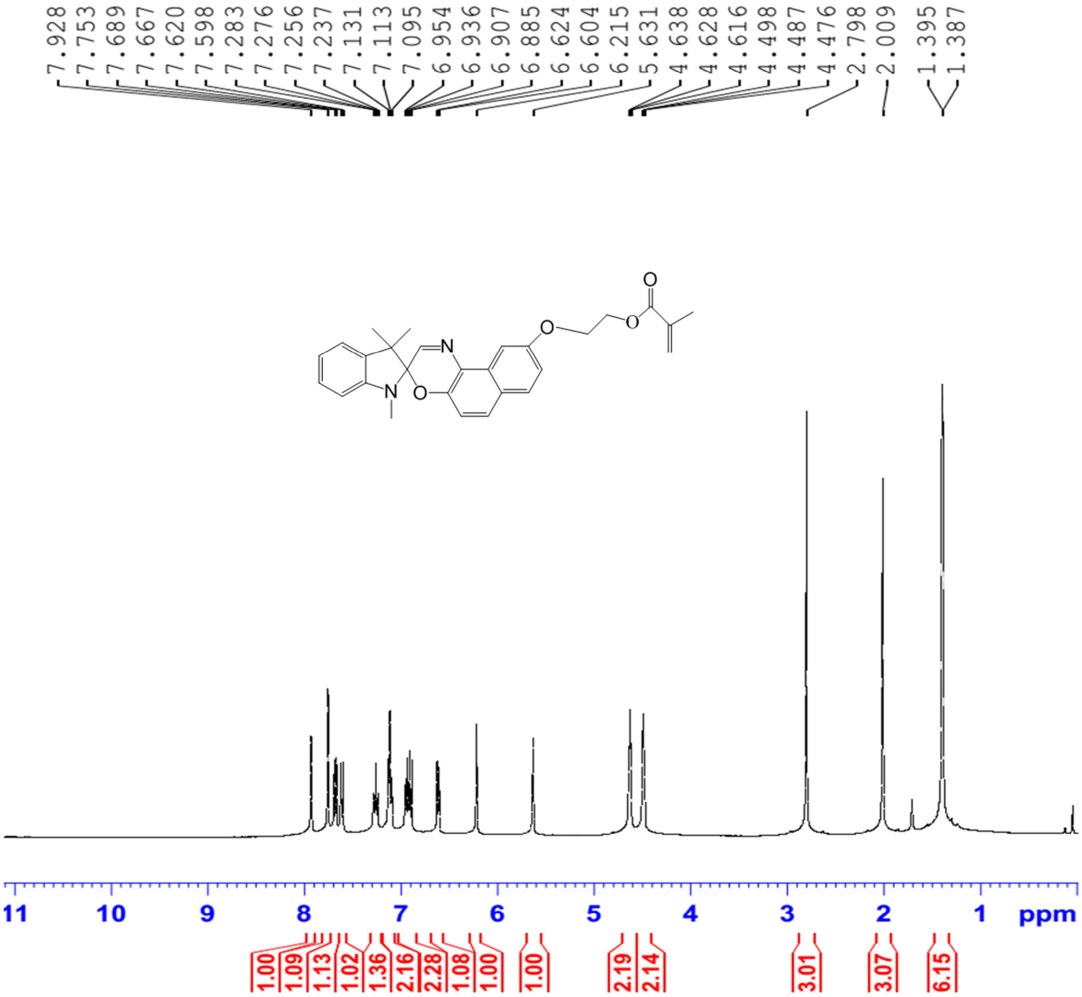

Fig. S1 ^{1}H NMR spectrum of SPO in $CDCl_3$

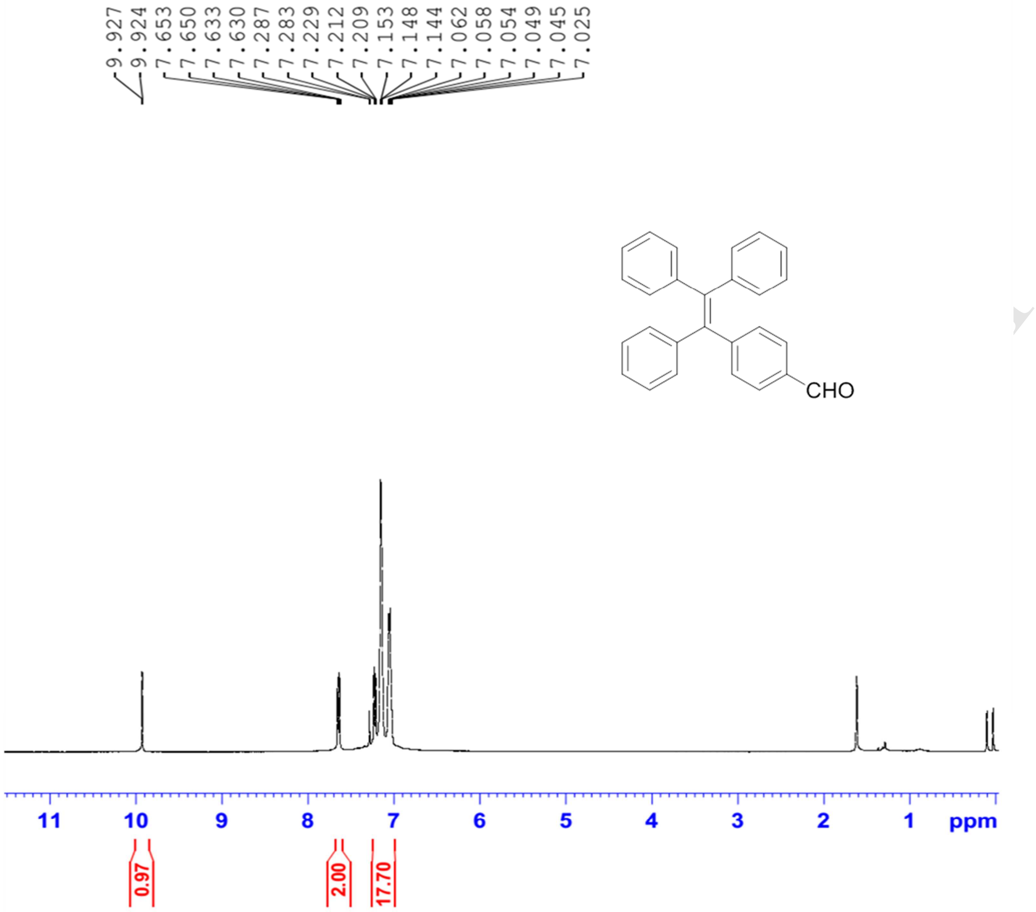

Fig. S2 ^{1}H NMR spectrum of TPE-CHO in $CDCl_3$

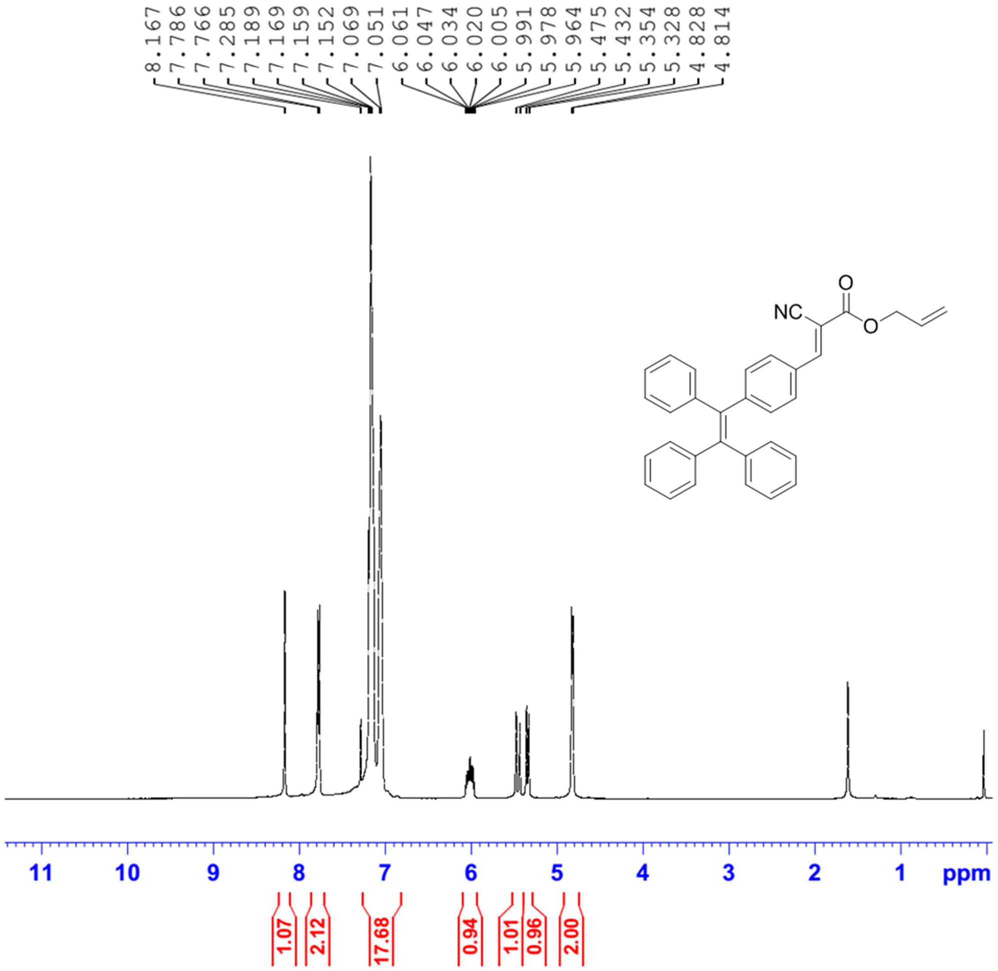

Fig. S3 ^{1}H NMR spectrum of TPE in $CDCl_3$

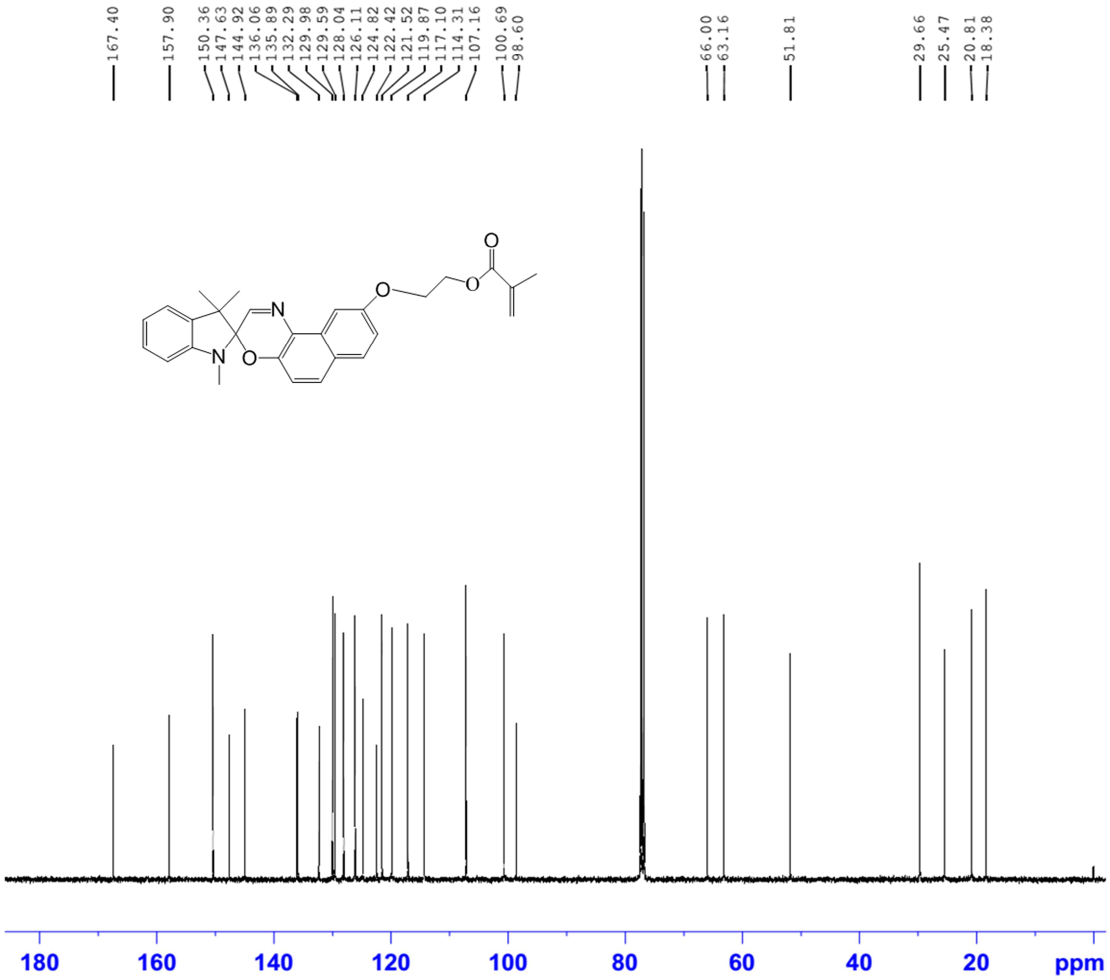

Fig. S4 ^{13}C NMR spectrum of SPO in CDCl$_3$

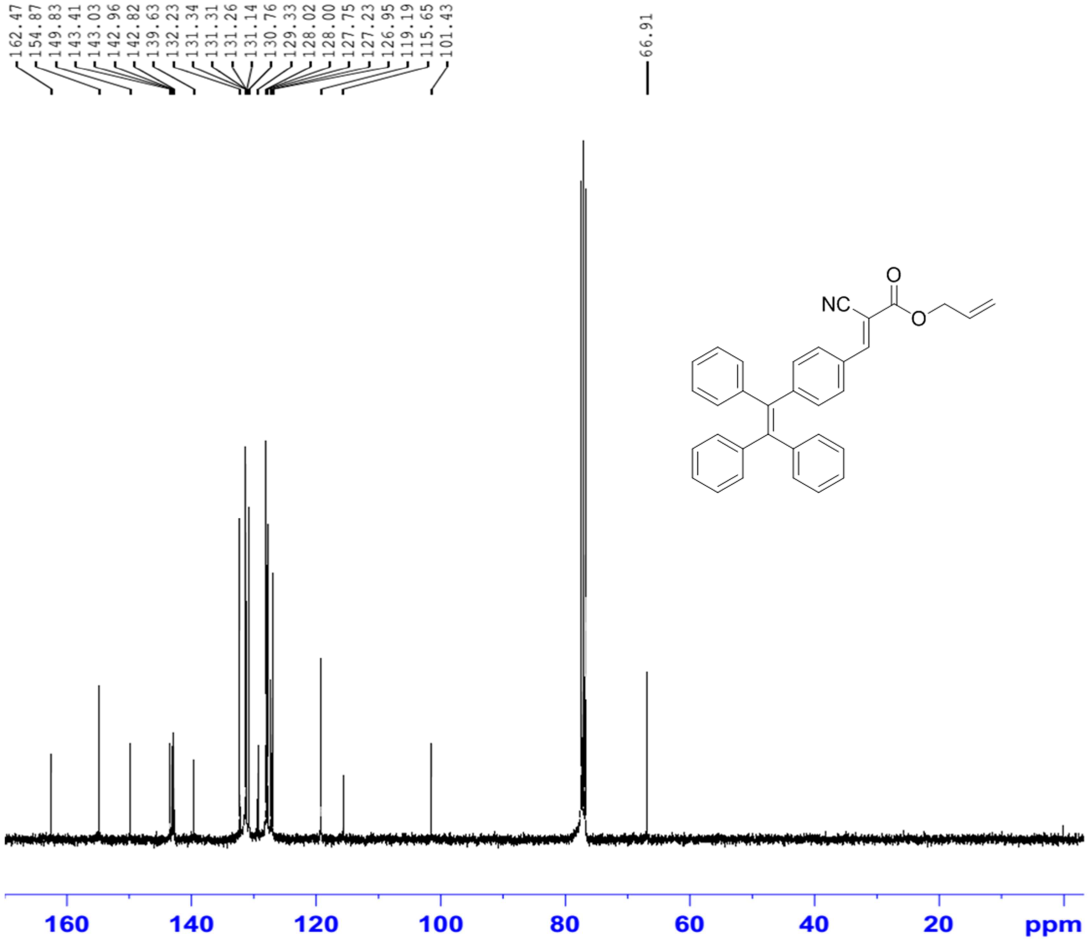

Fig. S5 ^{13}C NMR spectrum of TPE in $CDCl_3$

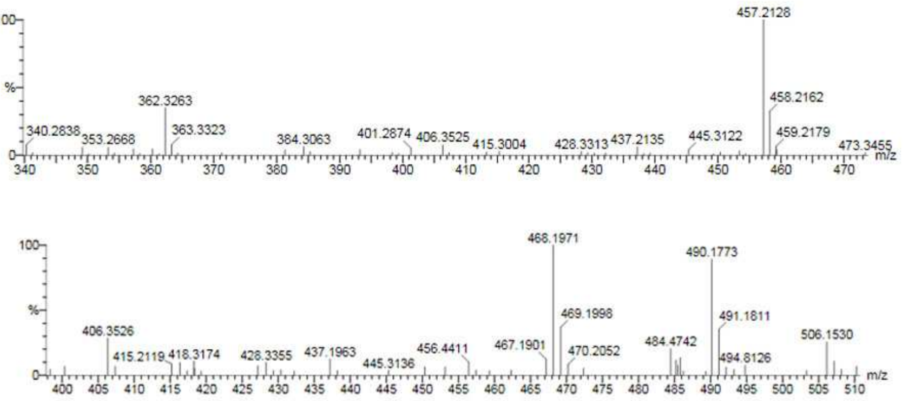

Fig. S6 HRMS spectra of SPO and TPE in CDCl$_3$

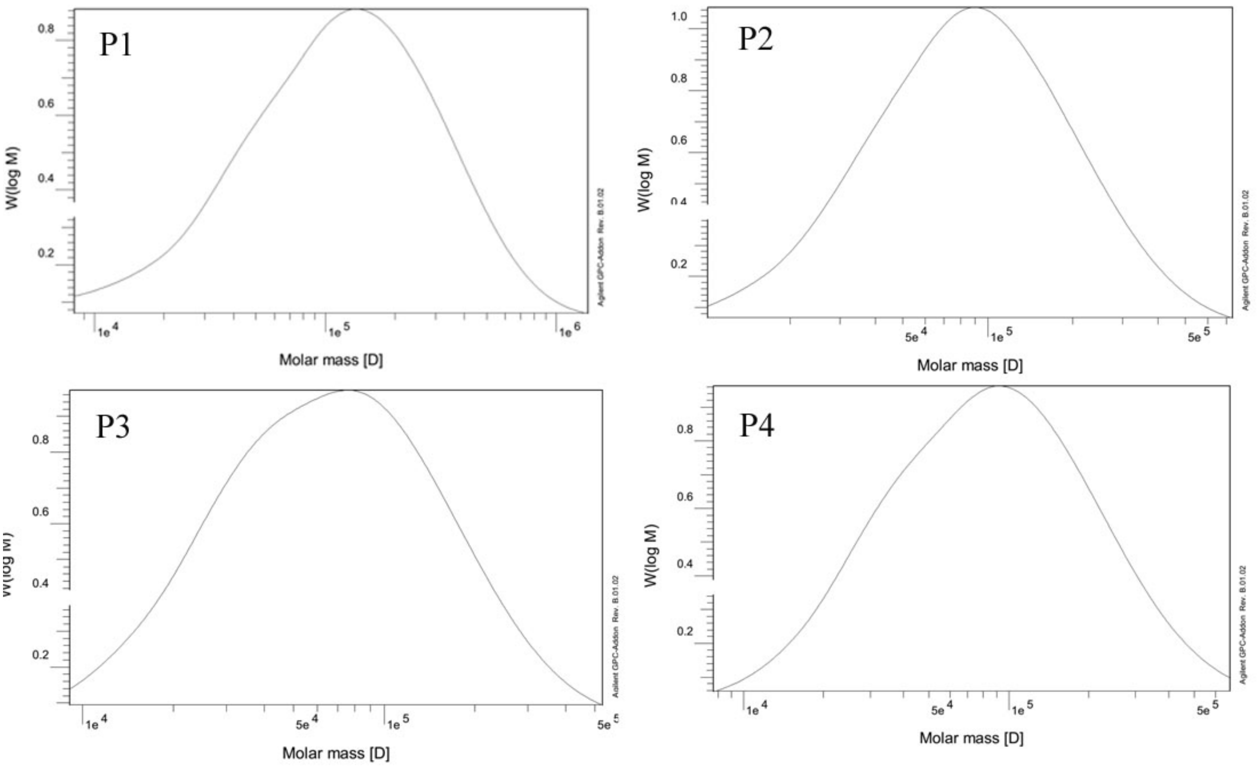

Fig. S7 The GPC chromatograms of **P$_1$**, **P$_2$**, **P3** and **P4**.

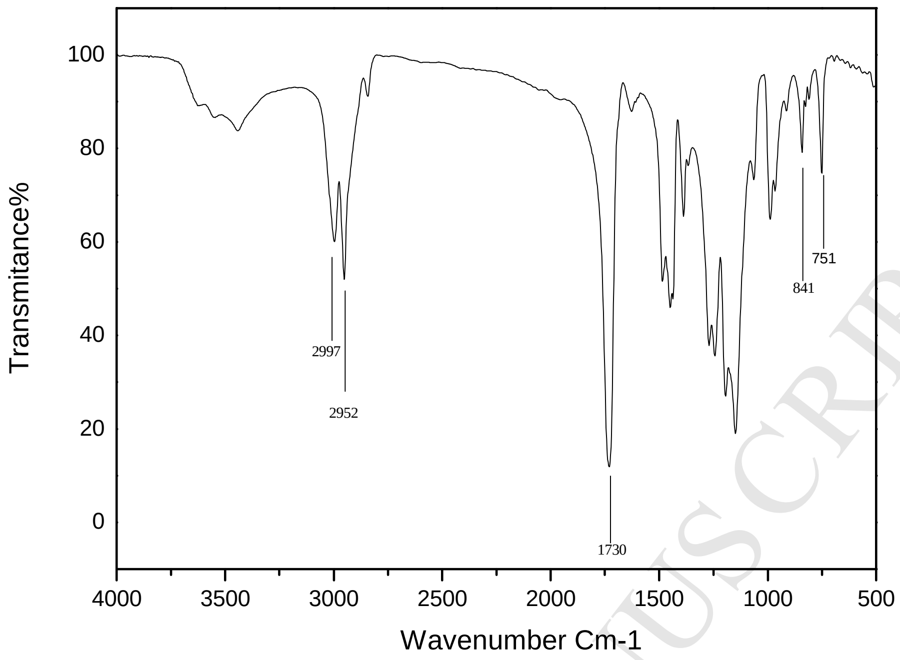

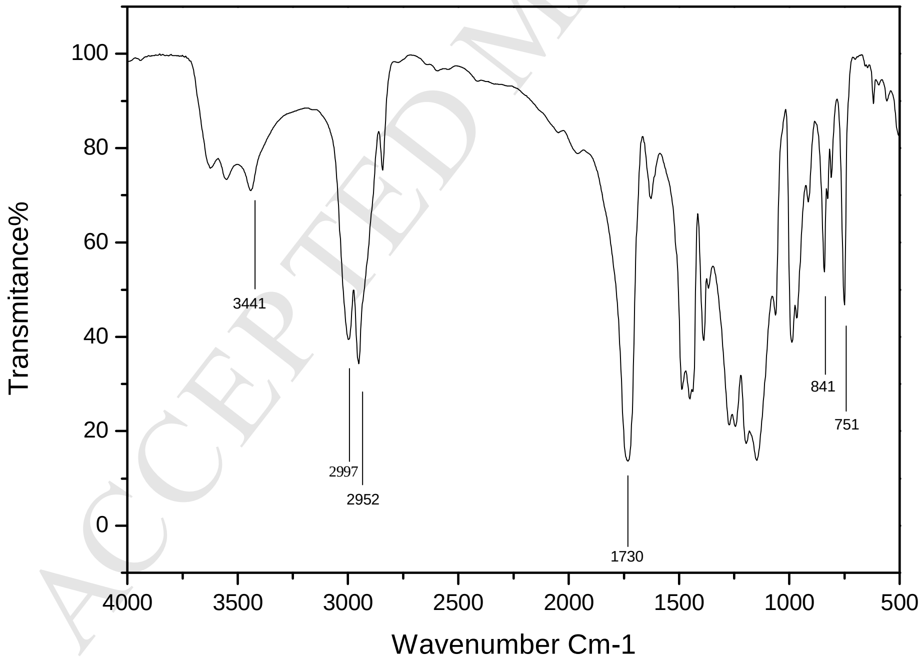

Fig S8. FTIR spectra of **P1** and **P2**

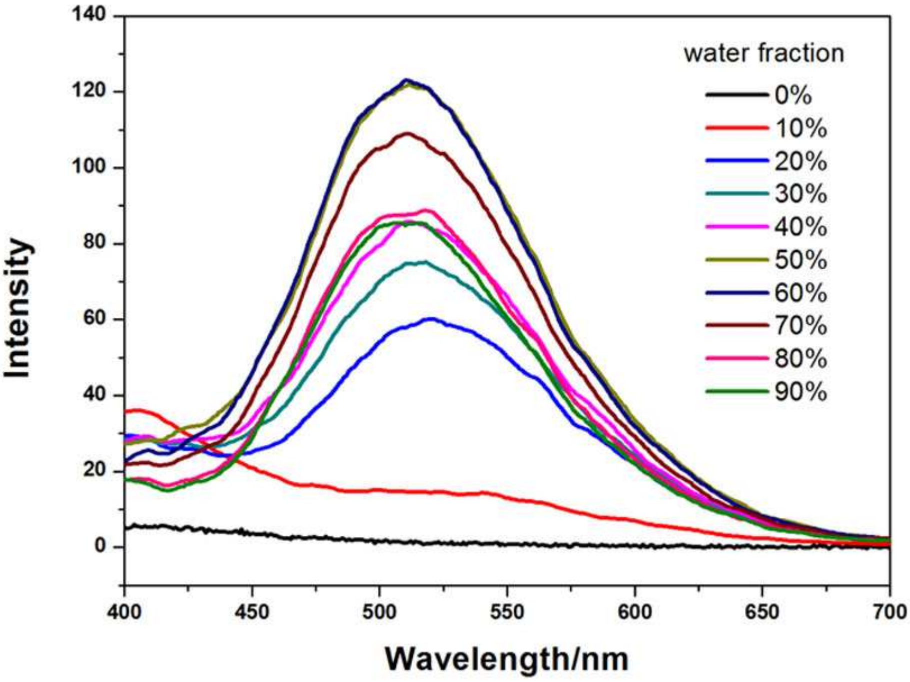

Fig.S9 PL spectra of **P3** in DMF/water mixtures with different water fractions, concentration 0.5mg/mL, λ_{ex} = 300 nm.

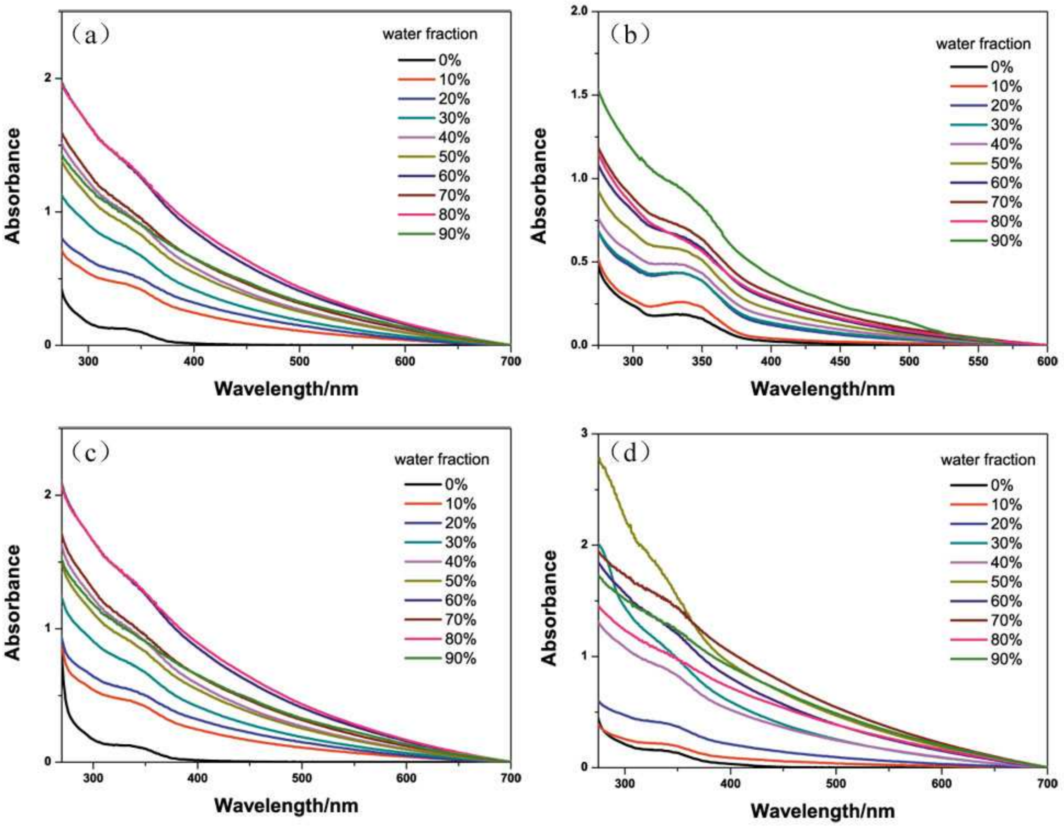

Fig.S10 Absorption spectra of **P1** (a), **P2** (b), **P3**(c) and **P4** (d) in different water-DMF (v/v) mixtures. Concentration:0.5mg/mL.